7902010018

CRACK ARREST TOUGHNESS DATA BASE FOR K_{IR}-CURVE

by

G. T. Hahn, P. C. Gehlen, R. G. Hoagland
J. Lereim and A. R. Rosenfield

INTRODUCTION

The K_{IR}-curve, specified in Section III of the ASME Boiler and Pressure Vessel Code is used in vessel integrity assessments to determine allowable pressures consistent with the postulated defect. The K_{IR}-curve (see Figure 1) reflects the variation of the lower bound of fracture toughness with temperature. The curve was defined in 1971 on the basis of then available measurements of several toughness parameters*. As shown in Figure 1, measurements of the crack arrest toughness figured prominently in the positioning of the K_{IR}-curve. Crack arrest values also enter into the crack propagation calculations specified in Section XI, Article A-5000 of the code. Since 1971, the understanding of crack arrest toughness and its measurement have been substantially refined. These developments have been applied in a program designed to provide a significant and more reliable body of crack arrest toughness measurements. This paper presents results for unirradiated A533B and A508B steel and a weldment. Crack arrest test specimens of a high copper weldment have been irradiated and will be tested in the near future.

CRACK ARREST MATERIAL PROPERTY

There is general agreement that a material's resistance to penetration by a fast moving crack may vary with crack velocity. This fracture resistance can be expressed in terms of the fast fracture toughness, K_{ID}, which is the stress intensity requirement to sustain the advancing crack tip. Figure 2 illustrates the possible variation of K_{ID} with crack velocity for a medium strength steel. The smallest value of stress intenstiy that can maintain continued crack propagation is equal to K_{Im}, the minimum toughness value on the K_{ID}-crack velocity

*These included the conventional fracture toughness parameter K_{Ic}, the high loading rate toughness K_{Id} and now called $K_{Ic}(\dot{K})$, and the crack arrest toughness K_{Ia} and now called K_{Im}.

7902010018

curve.* The minimum toughness is a measure of the crack stopping capacity of the material because crack arrest must occur under LEFM conditions when the instantaneous stress intensity is reduced below the minimum toughness value. Studies of 2 heats of A533B at temperatures between RT_{NDT} + 17 C and RT_{NDT} - 66 C, which facilitate the study of a wide range of crack velocities, point to the existence of a shallow, flat bottomed toughness minimum extended from a crack velocity of about 300 ms^{-1} to 900 ms^{-1}.

CRACK ARREST TEST PROCEDURE

The general strategy for conducting K_{Im}-measurements is outlined in Figure 3. Two essentially similar methods implementing this strategy have been proposed to ASTM by workers from Battelle and Materials Research Laboratory, Inc. The 2 test methods and an ongoing Cooperative Test Program involving 30 different laboratories are described more fully in the following paper. The present study employed the Battelle method:

- Duplex-DCB (140 x 380 x 50mm) and duplex-compact (254 x 247 x 50mm) test specimens (see Figure 4)
- Transverse wedge loading (see Figure 5)
- Measurement of the load point displacement existing at the onset of fast fracture and after arrest. These 2 displacements are essentially the same because of the stiff wedge loading (see Figure 6)
- Measurement of the size of the crack jump after arrest with the aid of heat tinting (Figure 7).

The value of K_{Im} is defined using the reference curves of Figure 8 which are the result of dynamic finite difference analyses; the value of K_{Ia} is obtained using the conventional static LEFM analysis. The assumptions implicit in the 2 analyses are given in Figure 9. While the authors regard the dynamic analysis more reliable than the static interpretation, this remains controversial and both sets of results are presented here.

---

*It has been recommended by the ASTM Dynamic Initiation and Crack Arrest Task Group E 24.03.04 that the minimum value be designated as the crack arrest toughness, K_{Im}. It should also be noted that the symbol K_{Ia}, which is frequently used to designate estimates of the crack arrest toughness obtained from a static analysis, appears in Section XI of the code since this section predates more recent dynamic analyses of crack arrest.

DATA BASE MATERIALS AND TESTING CONDITIONS

Crack arrest measurements were performed on 3 heats of A533B, 3 heats of A508, and a submerged arc weldment. These materials are described in Figure 10. The test temperatures were in the range from RT_{NDT}, to RT_{NDT} + 100 C. The steady state crack velocities produced in these tests are in the range 350 ms^{-1} to 750 ms^{-1}.

Test specimens of a high copper weldment (see Figure 10) described in Figure 11 have been irradiated to 10^{19} nvt and will be tested in the next quarter.

RESULTS OF K_{Im} AND K_{Ia} MEASUREMENTS

The results of the dynamic LEFM analyses of the crack arrest tests (K_{Im}-values) are summarized in Figures 12 and 13, the results of the static interpretation (K_{Ia}-values) are given in Figure 14. These figures illustrate the temperature dependence of the crack arrest toughness. They also show how well heat-to-heat variations can be described by a simple RT_{NDT} or NDT shift. Taken together, the K_{Im}-results indexed with respect to RT_{NDT} in Figure 12 show a significant spread reflecting variability within the different heats, as well as the variability from heat-to-heat not accounted for by the RT_{NDT} shift. Comparison with Figure 13 shows that indexing on NDT tends to reduce the data spread. The K_{Im}-values calculated from measurements reported by the Materials Research Laboratory and obtained using the alternative test method fall within the same scatter band. The comparisons with the K_{Ic}-values for these same heats* and the K_{IR}-curve reveal the following important points:

(i) At the RT_{NDT} the K_{Im}-values are about equal to K_{Ic}. The K_{Im}-values tend to increase more slowly with temperature than K_{Ic} above RT_{NDT}, but they remain well above the level of $K_{Ic}(\dot{K})$-values which is close to the K_{IR}-curve.

(ii) The K_{Im}-values for the A533 and A508 plates are considerably above K_{IR} demonstrating a sizable element of conservatism in the K_{IR}-curve as a design criterion. While the crack arrest values for the SA-weldment were substantially lower than the base plate, even the weldment K_{Im}-values fall significantly above the K_{IR}-curve.

---

*The average trend of K_{Ic}-values for the different heats is indicated in Figures 12-14 by the curve labeled (slow loading) K_{Ic}.

(iii) The K_{Ia}-values are on average 32 % smaller than the corresponding K_{Im}-values for these materials. Still, all the K_{Ia}-values for the base plates lie above the K_{IR}-curve, while the lower values for the weldment straddle the K_{IR}-curve. It should be noted that these results also reflect conservatism because K_{Ia}-values tend to understate the crack arrest toughness.

Fractographic studies indicate that the relatively high K_{Im}-levels displayed by the base plates can be traced to uncoordinated, out-of-plane crack front movement, which tends to produce a rough fracture surface, ductile ligaments and regions of high energy ductile shear failure (see Figures 15-17).

APPLICATION

In addition to the support they provide for the K_{IR}-curve, the crack arrest toughness values make it possible to assess the likelihood of crack arrest when the onset of rapid fracture cannot be precluded. Such assessments can be performed using conventional static LEFM analyses as illustrated in Figure 18a and c.

- A lower bound estimate of the extent of fracture can be obtained by assuming all the excess (kinetic) energy released in the process of crack extension (shaded area in Figure 18a) is dissipated prior to arrest. This assumption is valid in the limit of small crack jumps.
- An upper bound estimate is obtained by assuming all of the excess energy (shaded area 1 in Figure 18c) is conserved. This is a good approximation for crack jumps large relative to the component dimensions.

The report of the PVRC/MPC Task Group on Fracture Toughness Properties of Nuclear Components* notes that the crack arrest methodology in Section XI of the Code, which is based on the small jump-static analysis approach, is likely to be valid for less than 1-inch extensions in a vessel. This conclusion is supported by a dynamic analysis of a run arrest event in a thermally stressed cylinder produced by Cheverton and coworkers at ORNL. Methods of performing dynamic analyses of run arrest events in cylinders subjected to thermal stresses are currently being perfected at Battelle with the aim of establishing analytical procedures for large crack extensions.

*PVRC/MPC Report dated August 1973.

REFERENCES

"Fast Fracture and Crack Arrest Toughness of Reactor Pressure Vessel Steels", G. T. Hahn, R. G. Hoagland, J. Lereim, C. W. Marschall, and A. R. Rosenfield, to be presented at the ASTM Symposium on Crack Arrest Methodology and Applications, Philadelphia, November 6-7, 1978.

"Crack Arrest Concepts and Applications", G. T. Hahn, A. R. Rosenfield, C. W. Marschall, R. G. Hoagland, P. C. Gehlen, and M. F. Kanninen, presented at the Conference on Fracture and Fatigue Mechanics, Washington, D. C., September, 1978.

"Analysis of Crack Arrest in Reactor Pressure Vessels", R. G. Hoagland, P. C. Gehlen, A. R. Rosenfield, and G. T. Hahn, presented at the Joint ASME/CSME Pressure Vessels & Piping Conference, Montreal, Canada, June, 1978, ASME Publication No. 78-Mat-16.

Fast Fracture and Crack Arrest, ASTM STP 627, editors Hahn/Kanninen, July, 1977.

"Dynamic Analysis of Crack Propagation and Arrest in DCB Test Specimen", M. F. Kanninen, C. Popelar, and P. C. Gehlen, ASTM Symposium Fast Fracture and Crack Arrest, ASTM STP 627, July, 1977, p. 19.

"A Crack Arrest Measuring Procedure for K_{Im}, K_{ID}, and K_{Ia} Properties, R. G. Hoagland, A. R. Rosenfield, P. C. Gehlen, and G. T. Hahn, ASTM Symp. Fast Fracture and Crack Arrest, ASTM STP 627, July, 1977, p. 177.

"Fast Fracture Toughness of Steels", G. T. Hahn, R. G. Hoagland, and A. R. Rosenfield, Dynamic Fracture Toughness, Welding Institute, Abington, Cambridge, England, 1976, p. 237.

"Crack Branching in A533B Steel", G. T. Hahn, R. G. Hoagland, and A. R. Rosenfield, Fracture 1977, Vol. 2, ICF4, Waterloo, Canada, June, 1977.

"Crack Arrest and Its Relation to Propagating Crack Toughness, K_D", presented at the AIME Annual Meeting, March, 1977; submitted to Met. Trans.

Third Annual Progress Report (Contract No. AT(49-24)-0293), BMI-1995, May 1978.

11th Quarterly Progress Report (Contract No. AT(49-24)-0293), BMI-1980, May, 1978.

10th Quarterly Progress Report (Contract No. AT(49-24)-0293, BMI-1978, August, 1977.

Ninth Quarterly Progress Report (Contract No. AT(49-24)-0293), BMI-1970, NUREG -0289, July, 1977.

Eighth Quarterly Progress Report (Contract No. AT(49-24)-0293), BMI-1966, February, 1977.

Second Annual Progress Report (Task Agreement No. 62, Contract No. W-7405-eng-92), BMI-1959, October 1976.

Sixth Quarterly Progress Report (Task Agreement No. 62, Contract No. W-7405-eng-92), BMI-1951, July, 1976.

Fifth Quarterly Progress Report (Task Agreement No. 62, Contract No. W-7405-eng-92), BMI-1944, March, 1976.

Fourth Quarterly Progress Report (Task Agreement No. 62, Contract No. W-7405-eng-92), BMI-1939, November, 1975.

First Annual Progress Report (Task Agreement No. 62, Contract No. W-7405-eng-92), BMI-1937, August 1975.

Second Quarterly Progress Report (Task Agreement No. 62, Contract No. W-7405-eng-92), BMI-1934, May, 1975.

First Quarterly Progress Report (Task Agreement No. W-7405-eng-92), January, 1975.

Topical Report: R. G. Hoagland, M. F. Kanninen, A. R. Rosenfield, G. T. Hahn, "Rectangular-DCB Specimens for Fast Fracture and Crack Arrest Measurements", BMI-1933, December, 1974.

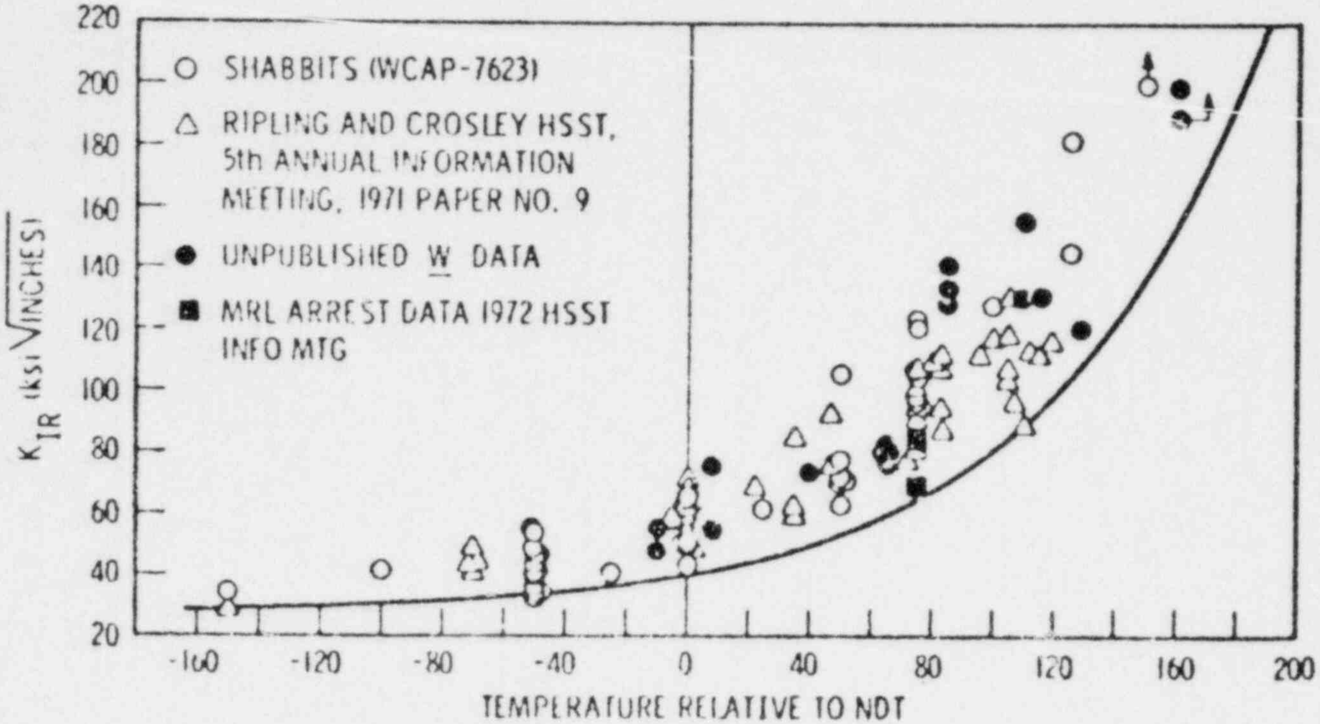

FIGURE 1. DERIVATION OF CURVE OF REFERENCE STRESS INTENSITY FACTOR, K_{IR} (AFTER WRC BULLETIN 175)

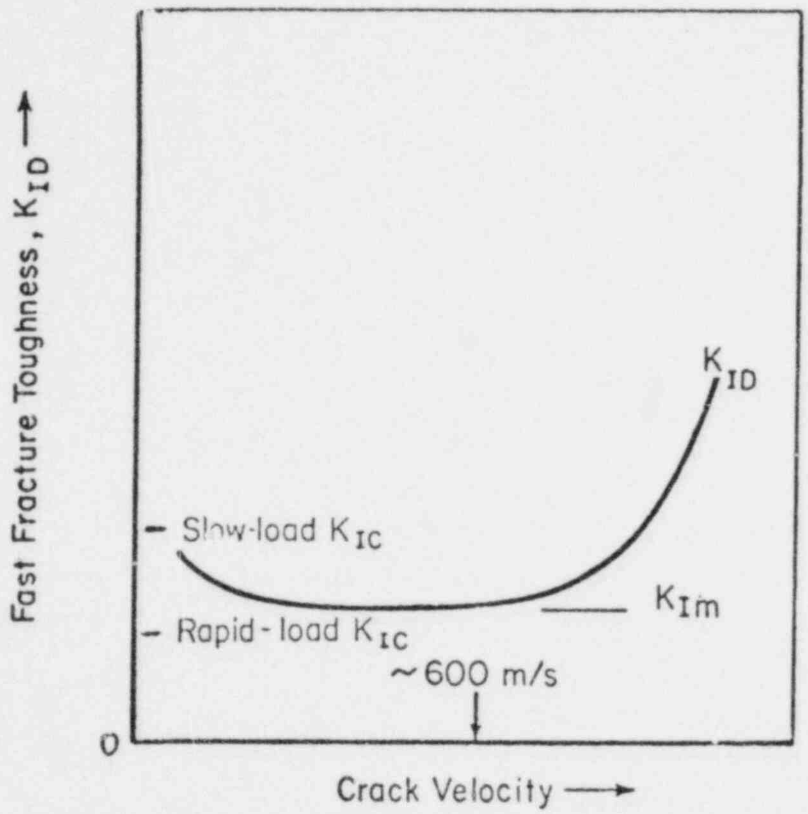

FIGURE 2. SCHEMATIC REPRESENTATION OF THE RESISTANCE TO PENETRATION BY A FAST MOVING CRACK. The resistance to extension of a stationary crack is the conventional slow load fracture toughness K_{Ic}. The curve illustrates a possible variation of the fast fracture toughness, K_{ID}, with crack velocity. The minimum toughness of the K_{ID}-crack velocity curve is K_{Im} which is called the crack arrest toughness. The assumed temperature is at or moderately above the RT_{NDT}. For comparison the level of K_{Ic} determined from rapidly loaded tests is shown for typical low-to-medium strength structural steels in this assumed temperature range.

FIGURE 3. FEATURES OF LEFM CRACK ARREST TESTING

1. <u>PRODUCE UNSTABLE FRACTURE EVENT</u>

   GENERATE K_I-LEVELS INITIALLY HIGHER THAN K_{IC} AND K_{IM} UNDER LEFM CONDITIONS

   -- *USE BLUNT NOTCH TOGETHER WITH HARDENED STARTER SECTION OR WELD EMBRITTLED SPECIMEN*

2. <u>ARREST CRACK</u>

   DESIGN SPECIMEN GEOMETRY AND LOADING TO GIVE DECREASING K_I-FIELD WITH CRACK EXTENSION

   -- *USE DCB OR COMPACT SPECIMEN WITH STIFF LOADING*

3. <u>PROMOTE FLAT, PLANE STRAIN FRACTURE</u>

   -- *USE FACE GROOVES*

4. <u>REDUCE SPECIMEN-TESTING MACHINE INTERACTION</u>

   -- *USE LONGITUDINAL OR TRANSVERSE WEDGE LOADING*

5. <u>SIMPLIFY MEASUREMENT AND ANALYSIS TASKS</u>

   -- *MEASURE LOAD POINT DISPLACEMENT AT ONSET OF FRACTURE OR AFTER ARREST AND CHANGE IN CRACK LENGTH (BY HEAT TINTING)*

   -- *USE TABLES OR REFERENCE CURVES DERIVED FROM STATIC OR DYNAMIC LEFM ANALYSES TO INTERPRET MEASUREMENTS*

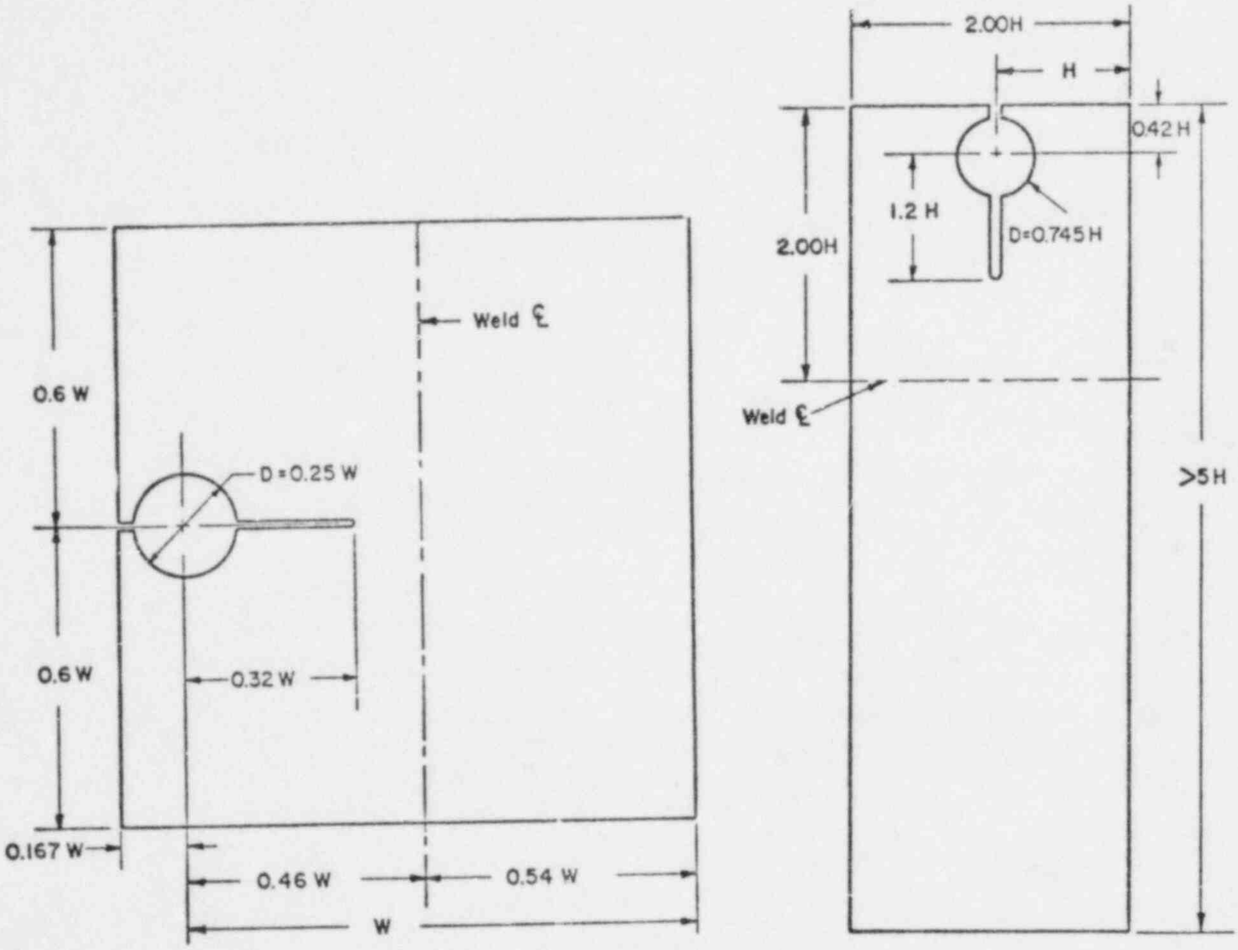

W = 212MM

H = 70MM

FIGURE 4. CRACK ARREST TEST SPECIMENS: (LEFT) DUPLEX-COMPACT AND (RIGHT) DUPLEX-DCB TEST SPECIMENS 50mm-THICK AND MACHINED WITH 45°, 6mm-DEEP FACE GROOVES (NOT SHOWN)

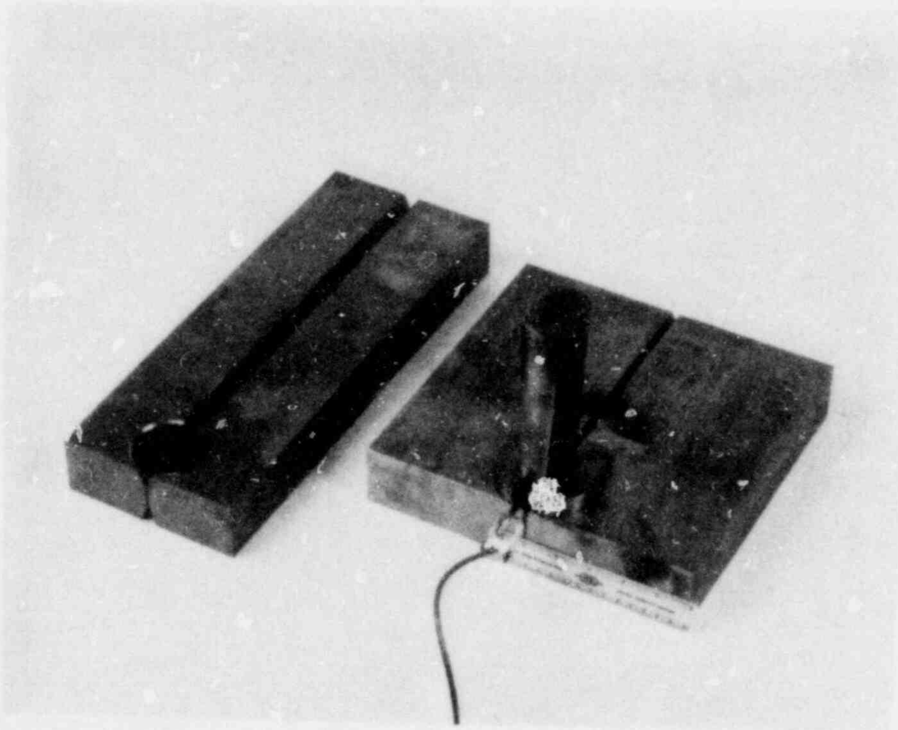

FIGURE 5. CRACK ARREST TEST SPECIMENS AND TRANSVERSE WEDGE LOADING ARRANGEMENT

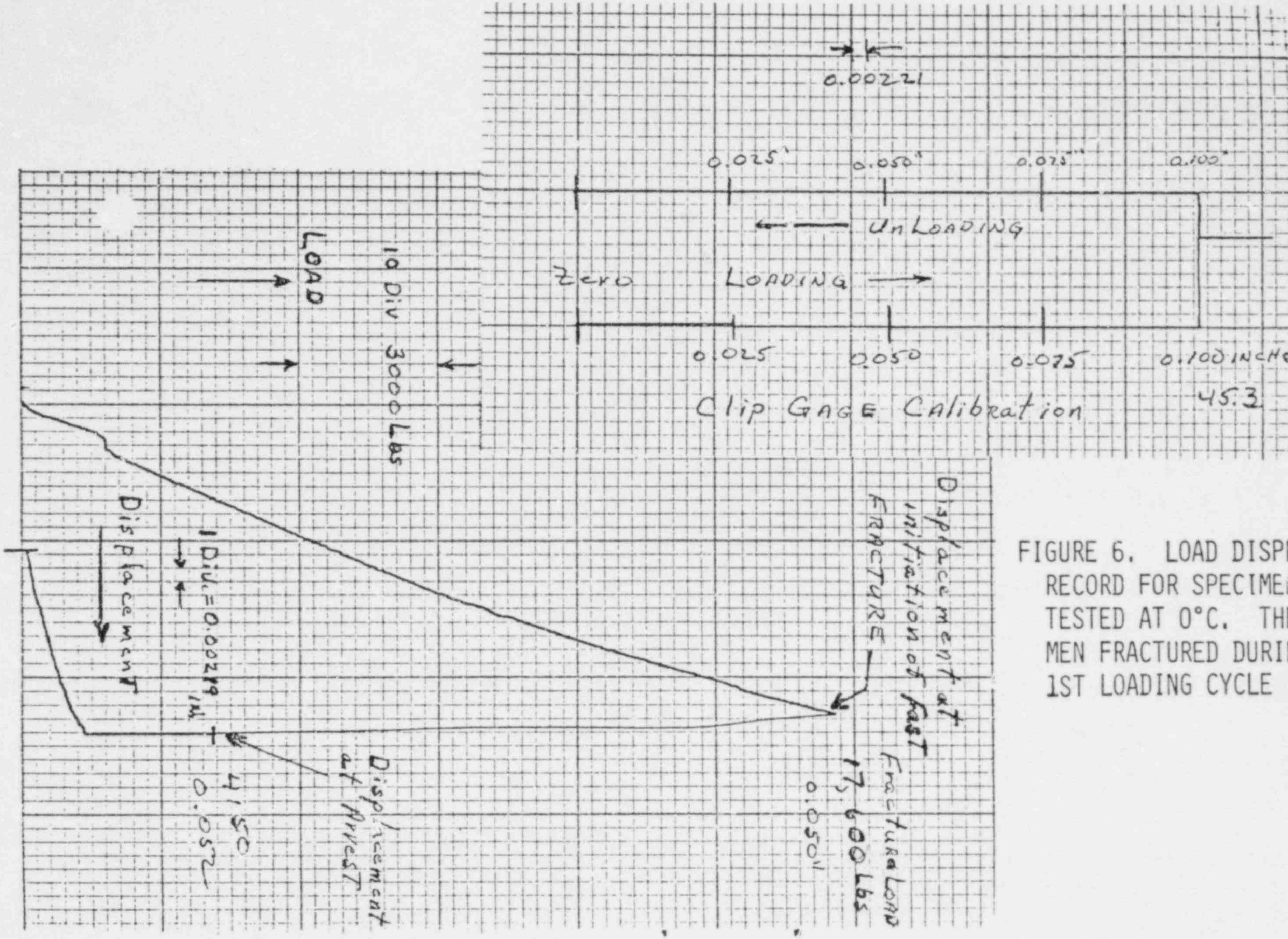

FIGURE 6. LOAD DISPLACEMENT RECORD FOR SPECIMEN RH-55 TESTED AT 0°C. THE SPECIMEN FRACTURED DURING THE 1ST LOADING CYCLE

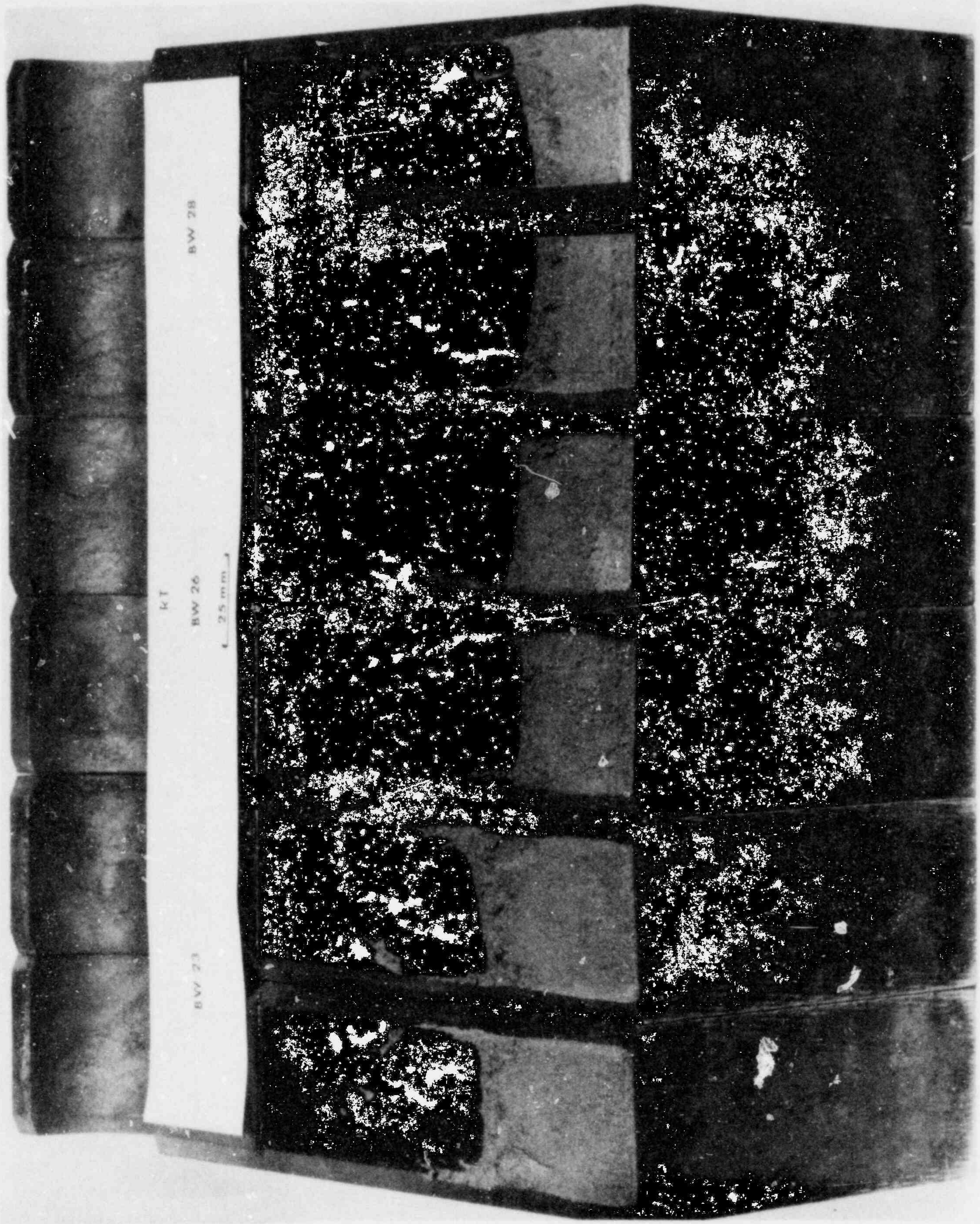

FIGURE 7. FRACTURED AND HEAT TREATED CRACK ARREST TEST SPECIMENS OF A508 STEEL

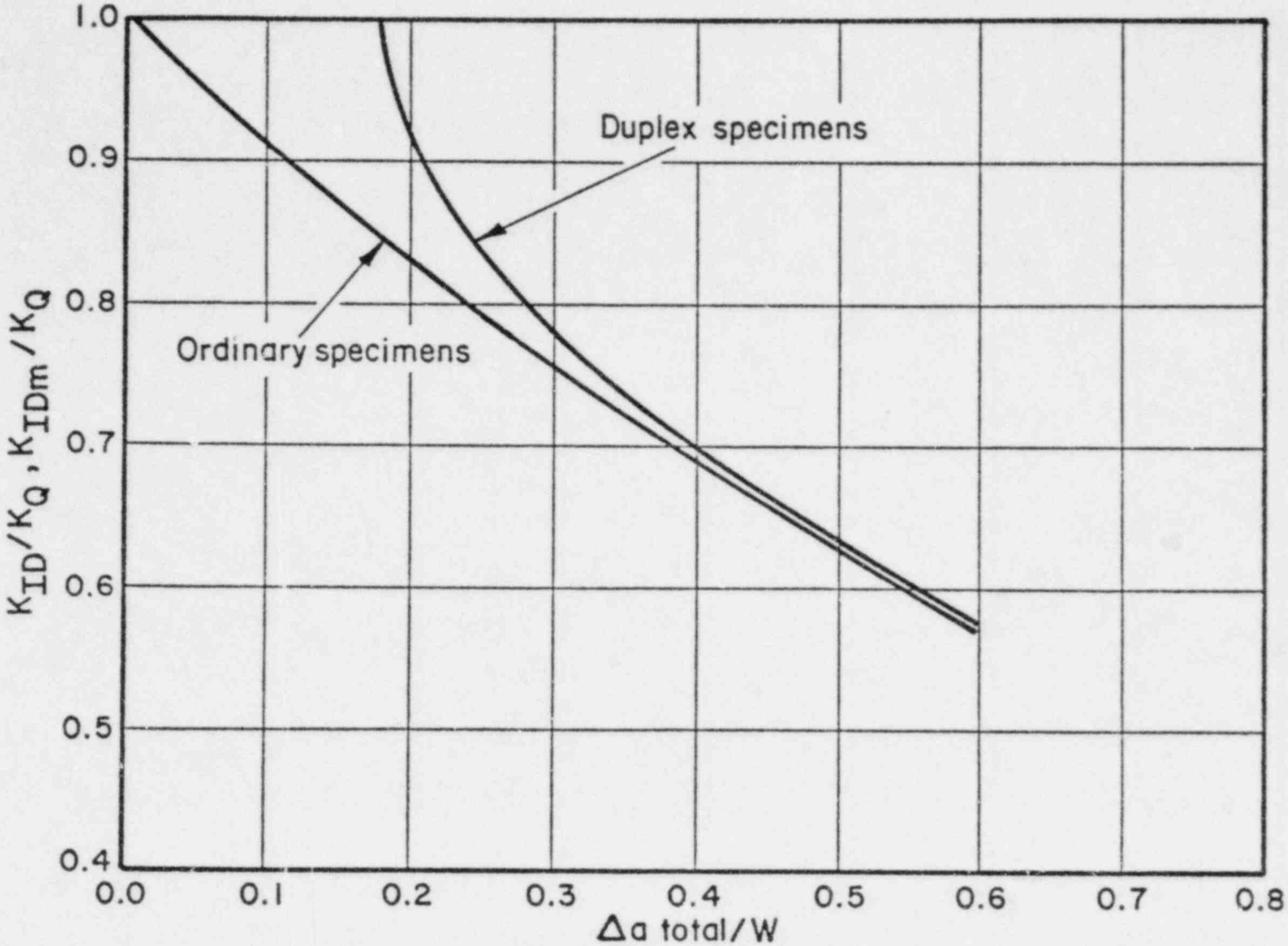

FIGURE 8. REFERENCE CURVES FOR ORDINARY AND DUPLEX-COMPACT TENSION TEST SPECIMENS SHOWING THE RELATION BE- BETWEEN $\Delta a/W$ AND K_{ID}/K_Q AND K_{ID}/K_Q

FIGURE 9: ANALYSIS OF CRACK ARREST MEASUREMENTS

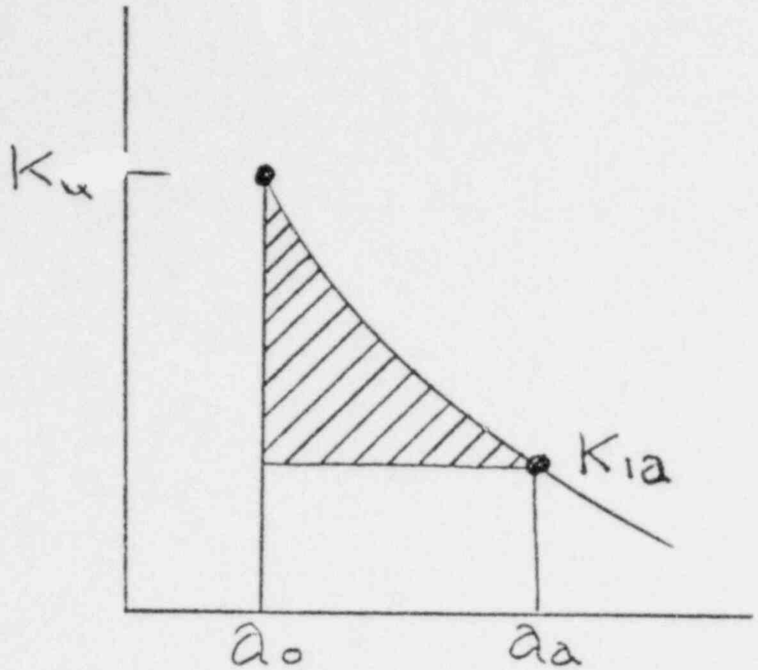

A. <u>STATIC APPROACH</u>

- DERIVES K_{IA} FROM LOAD POINT DISPLACEMENT VALUE AND CRACK LENGTH MEASURED AFTER ARREST
- USES STATIC LEFM ANALYSIS WHICH NEGLECTS INFLUENCE OF KINETIC ENERGY (SHADED AREA)
- ASSUMES KINETIC ENERGY DISSIPATION BY DAMPING IS COMPLETE PRIOR TO ARREST

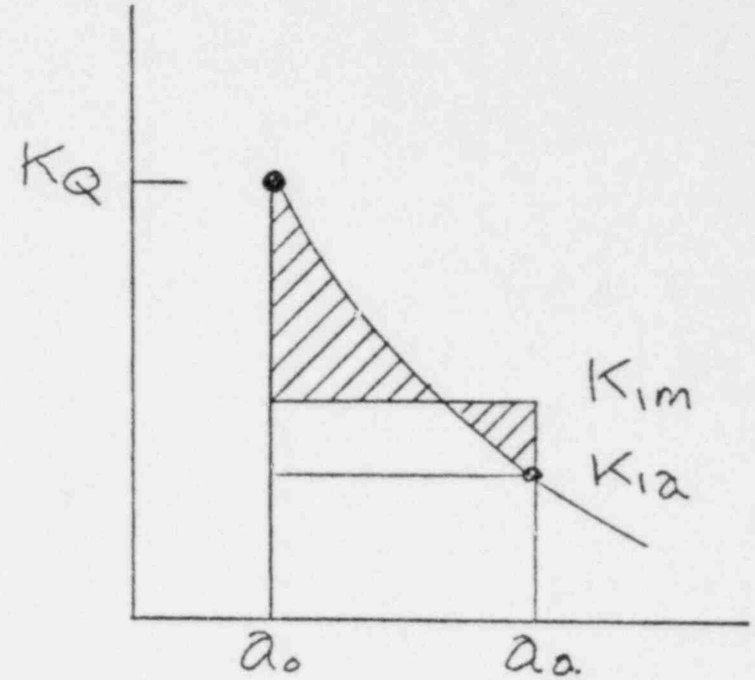

B. <u>DYNAMIC APPROACH</u>

- DERIVES K_{IM} FROM DISPLACEMENT VALUE AT ONSET OF FRACTURE AND CRACK LENGTH AT ARREST
- USES 2D, DYNAMIC LEFM ANALYSIS TO CALCULATE KINETIC ENERGY INFLUENCE
- ASSUMES KINETIC ENERGY DISSIPATION BY DAMPING PRIOR TO ARREST IS NEGLIGIBLE

FIGURE 10. DATA BASE MATERIALS

ALLOY	(HEAT)	NDT, C	RT_{NDT}, C	CVN(SHELF)FT/LBS
A533B	(BCL)	-12	-12	134
A533B	(CBI)	-29	-12	~ 90
A533B	(CE)	-12	-12	118
A533B	(CTP)	-40	-20	75
A508	(B&W/B)	7	- 7	120
A508	(B&W/D)	4	4	148
SA WELDMENT	(CE)	-57	-57	130
SA WELDMENT*	(BKS)	-46(80)**	-18(110)**	78(45)**

* HIGH COPPER/PHOSPHOROUS WELDMENT (Cu: 0.30, P: 0.014).

** VALUES AFTER IRRADIATION TO 1.10^{19} NVT.

FIGURE 11. ARRANGEMENT OF TEST SPECIMENS IN IRRADIATION CAPSULE

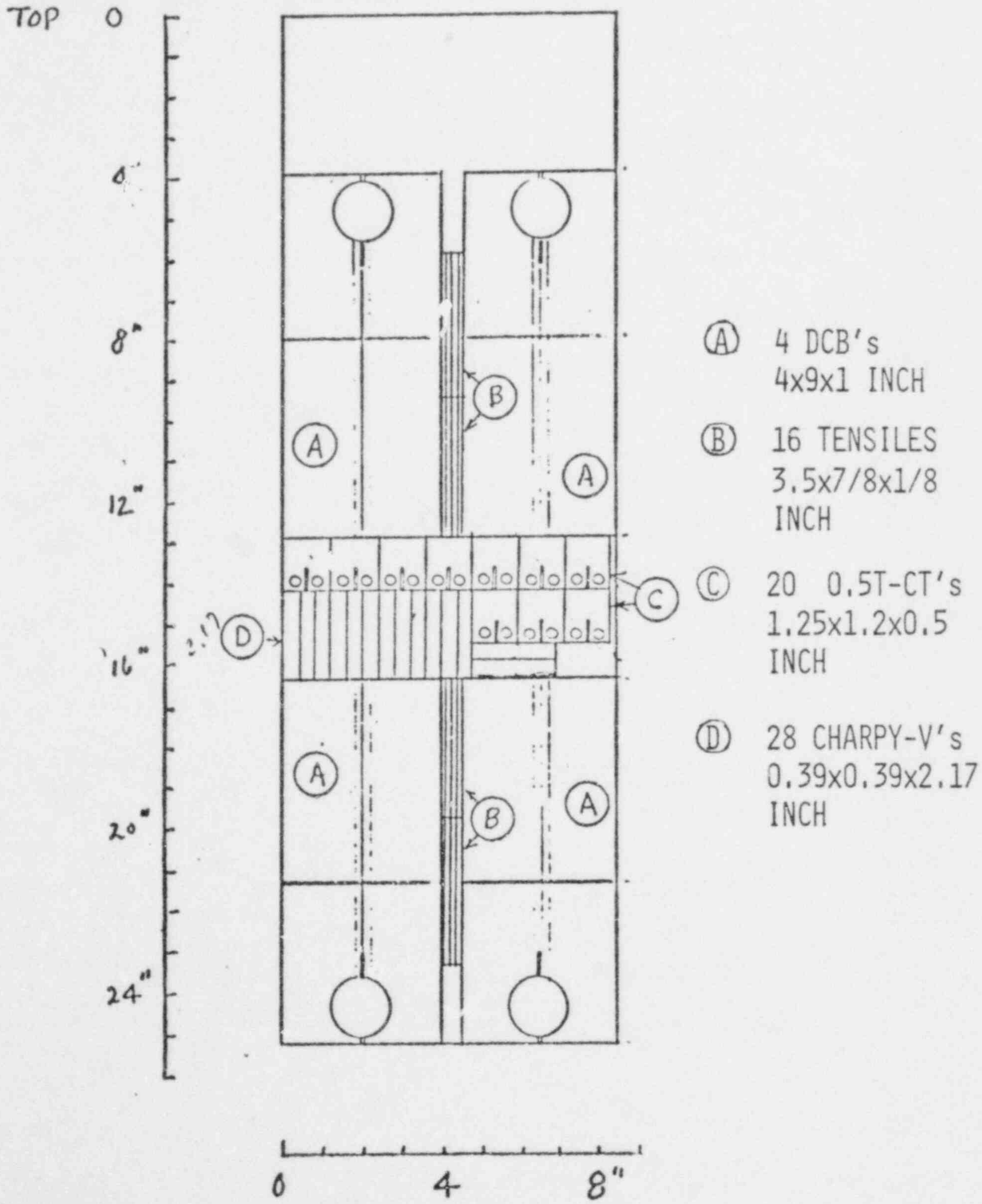

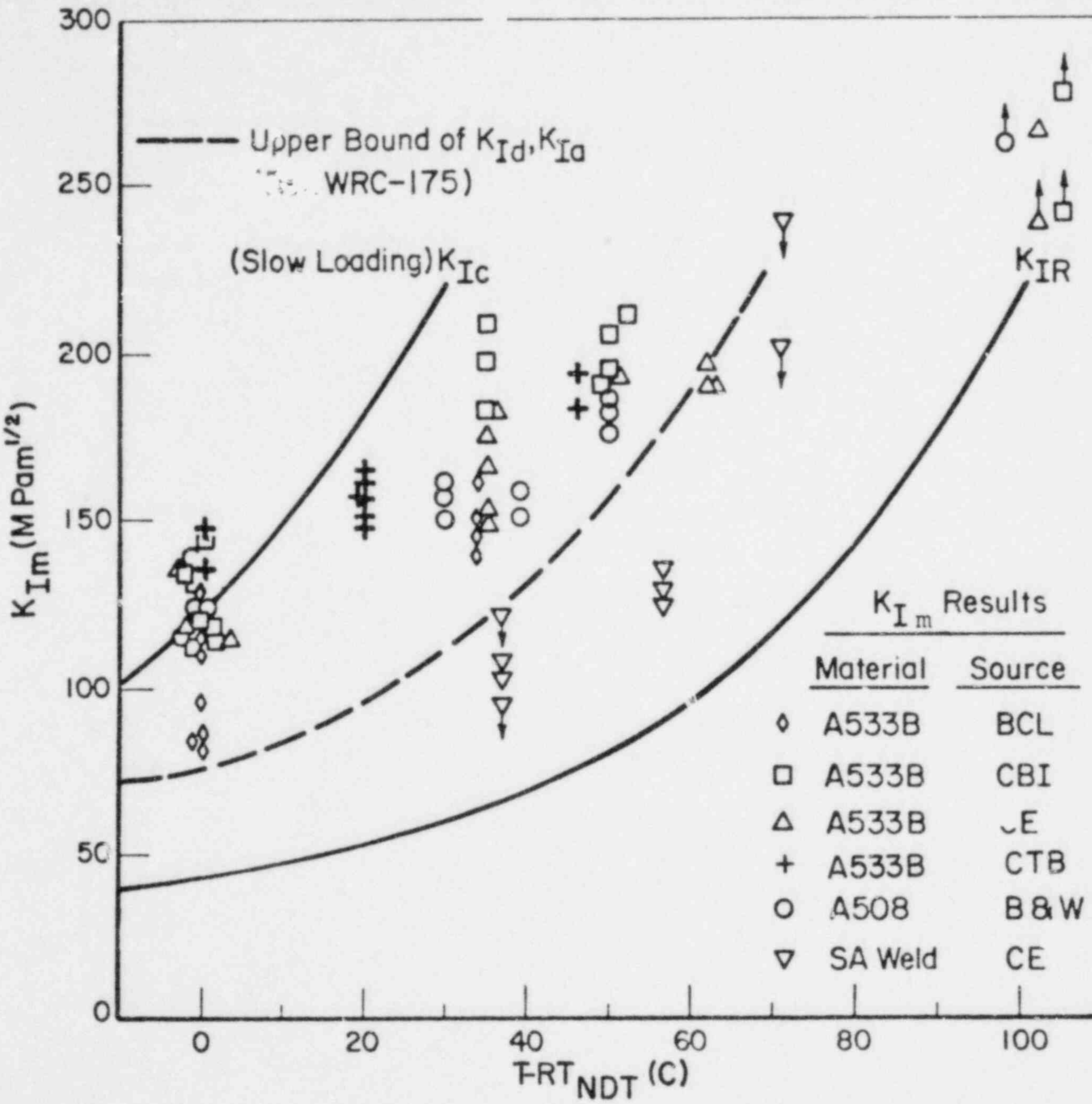

FIGURE 12. RESULTS OF CRACK ARREST TOUGHNESS MEASUREMENTS ON DATA BASE MATERIALS DERIVED FROM THE DYNAMIC ANALYSIS APPROACH AND INDEXED ON RT_{NDT}

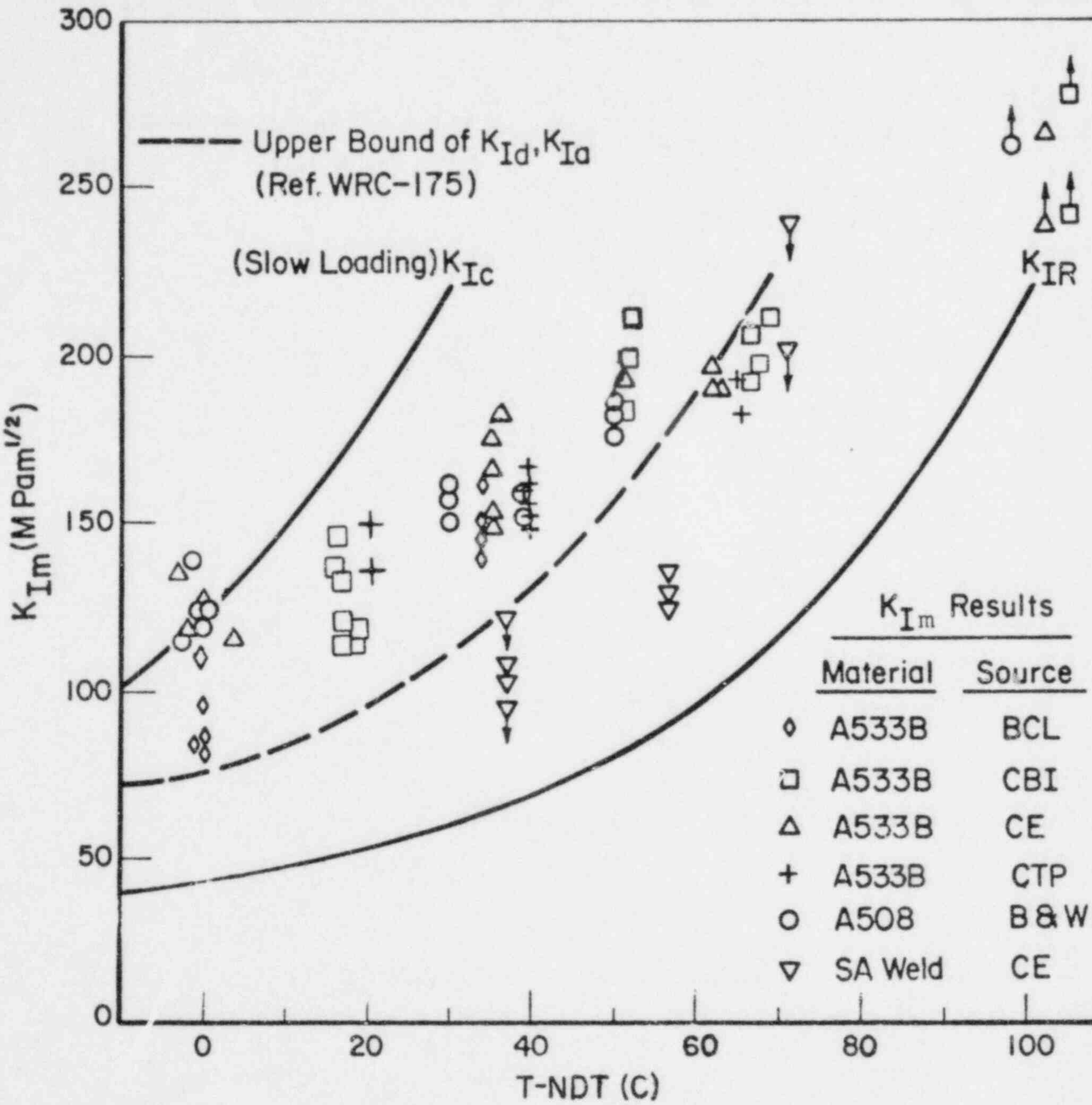

FIGURE 13. RESULTS OF CRACK ARREST TOUGHNESS MEASUREMENTS ON DATA BASE MATERIALS DERIVED FROM THE DYNAMIC ANALYSIS APPROACH AND INDEXED ON NDT

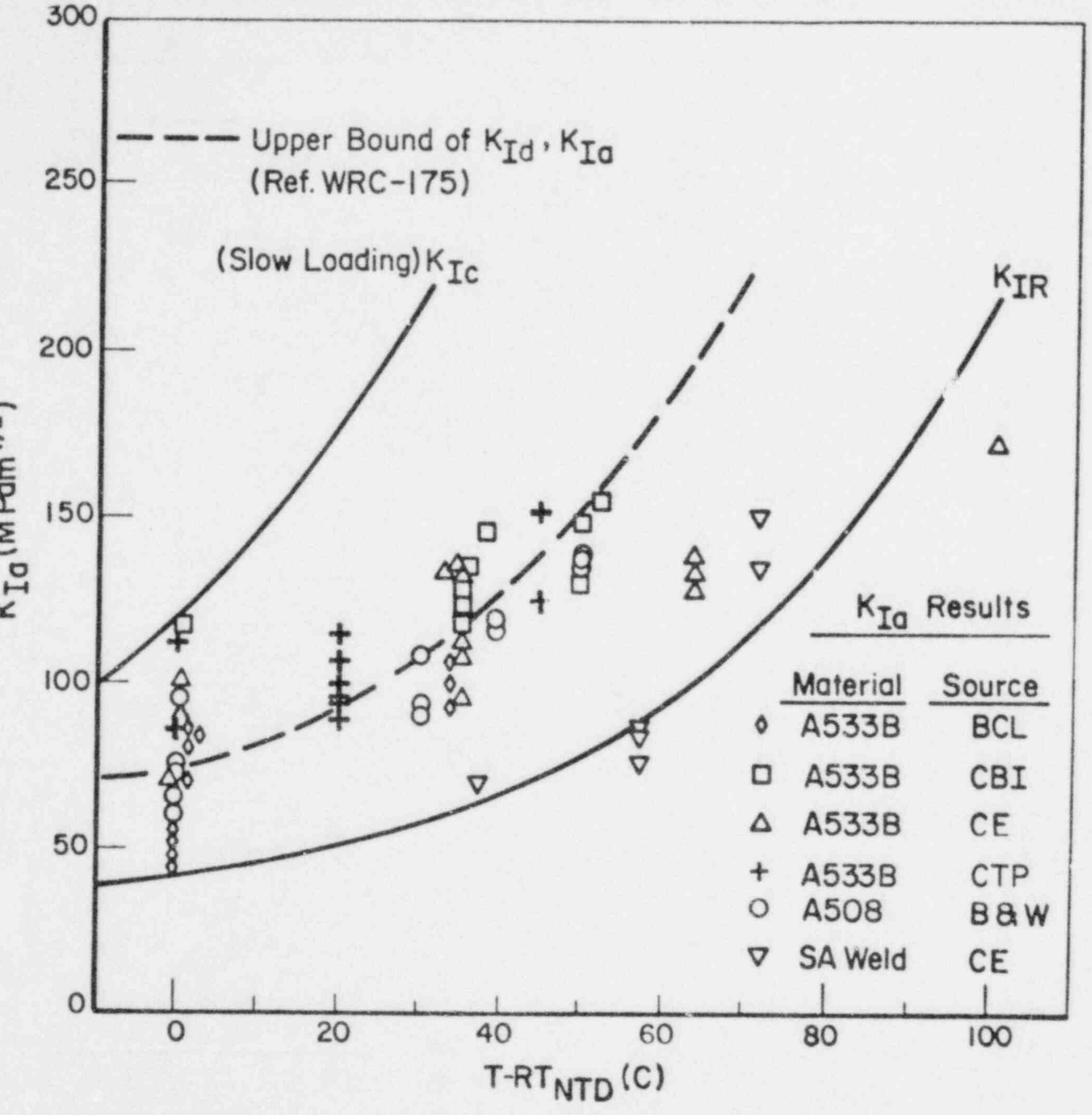

FIGURE 14. RESULTS OF CRACK ARREST TOUGHNESS MEASUREMENTS ON DATA BASE MATERIALS DERIVED FROM THE STATIC ANALYSIS APPROACH AND INDEXED ON RT_{NDT}

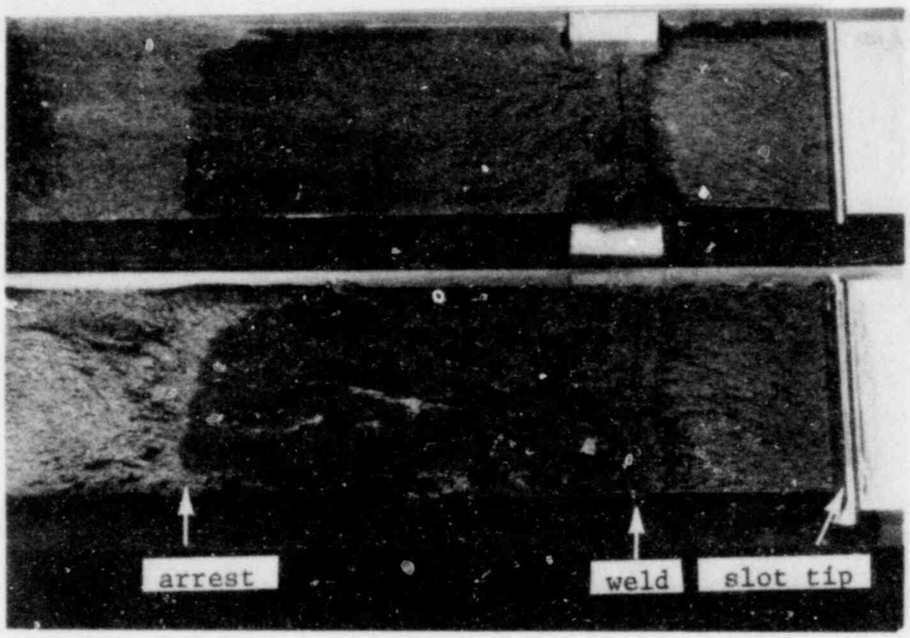

Figure 15. Appearance of fast fractures in 250 x 5υ mm duplex-compact crack arrest specimens of nuclear pressure vessel steel: (top) SA-weldment tested at RT_{NDT} + 57°C, K_{Im} = 127 $MPam^{1/2}$, (bottom) A508 tested at RT_{NDT} + 30°C, K_{Im} = 157 $MPam^{1/2}$. The fractures initiated in 4340 steel from the root of the blunt slot on the right side of the photograph, entered the test section at the weld (3-5 mm-wide electron beam weld), and arrested. The newly created surfaces were darkened by heat tinting, before breaking the specimens at -76°C to expose the fractures. The light (unoxidized) regions behind the crack front are ligaments which were unbroken when the crack arrested

FIGURE 16. CONSEQUENCES OF OUT OF PLANE CRACK FRONT MOVEMENT

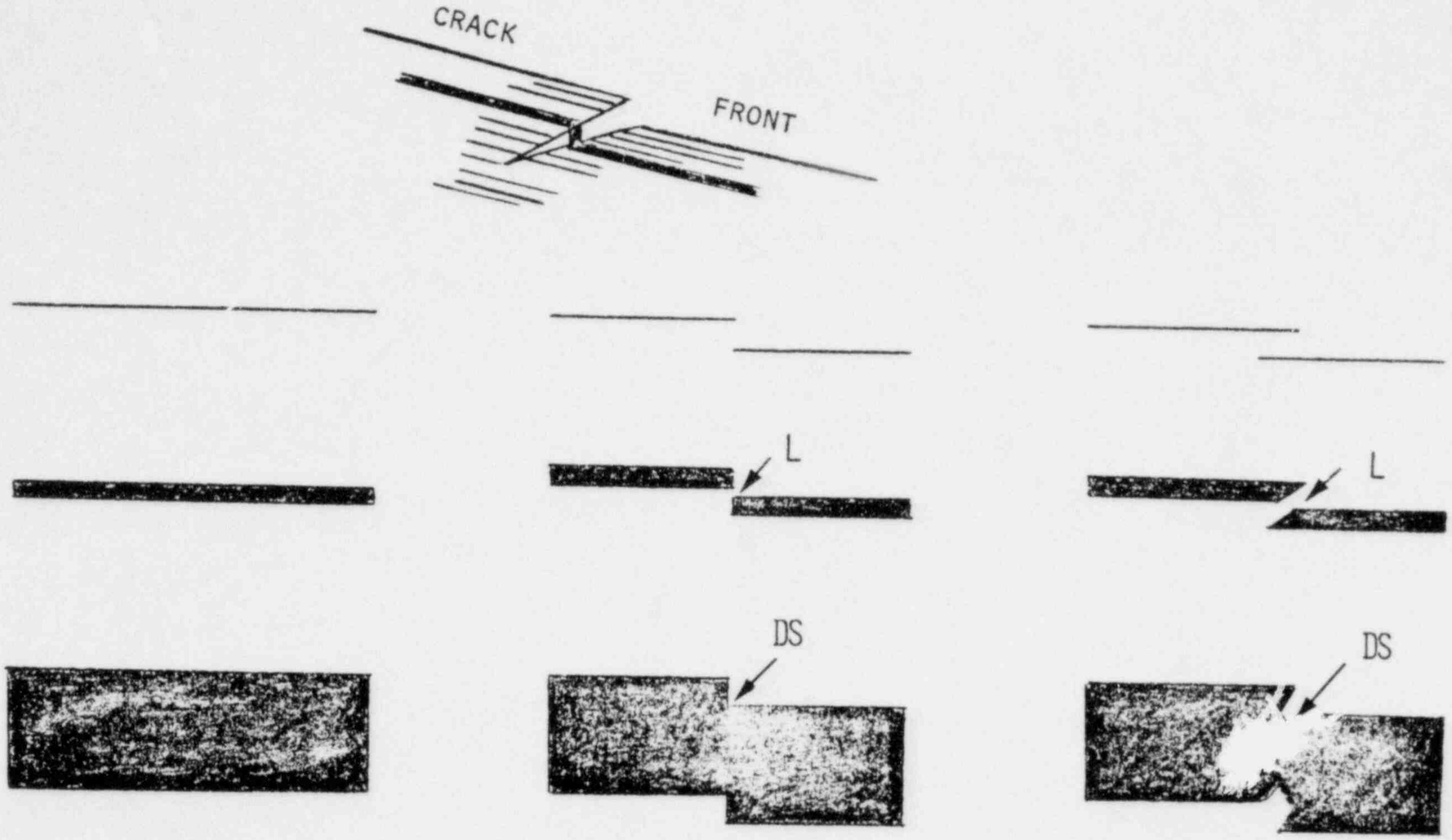

A. NO OUT-OF-PLANE MOVEMENT

B. OUT-OF-PLANE MOVEMENT

C. OUT-OF-PLANE MOVEMENT WITH UNDERCUTTING

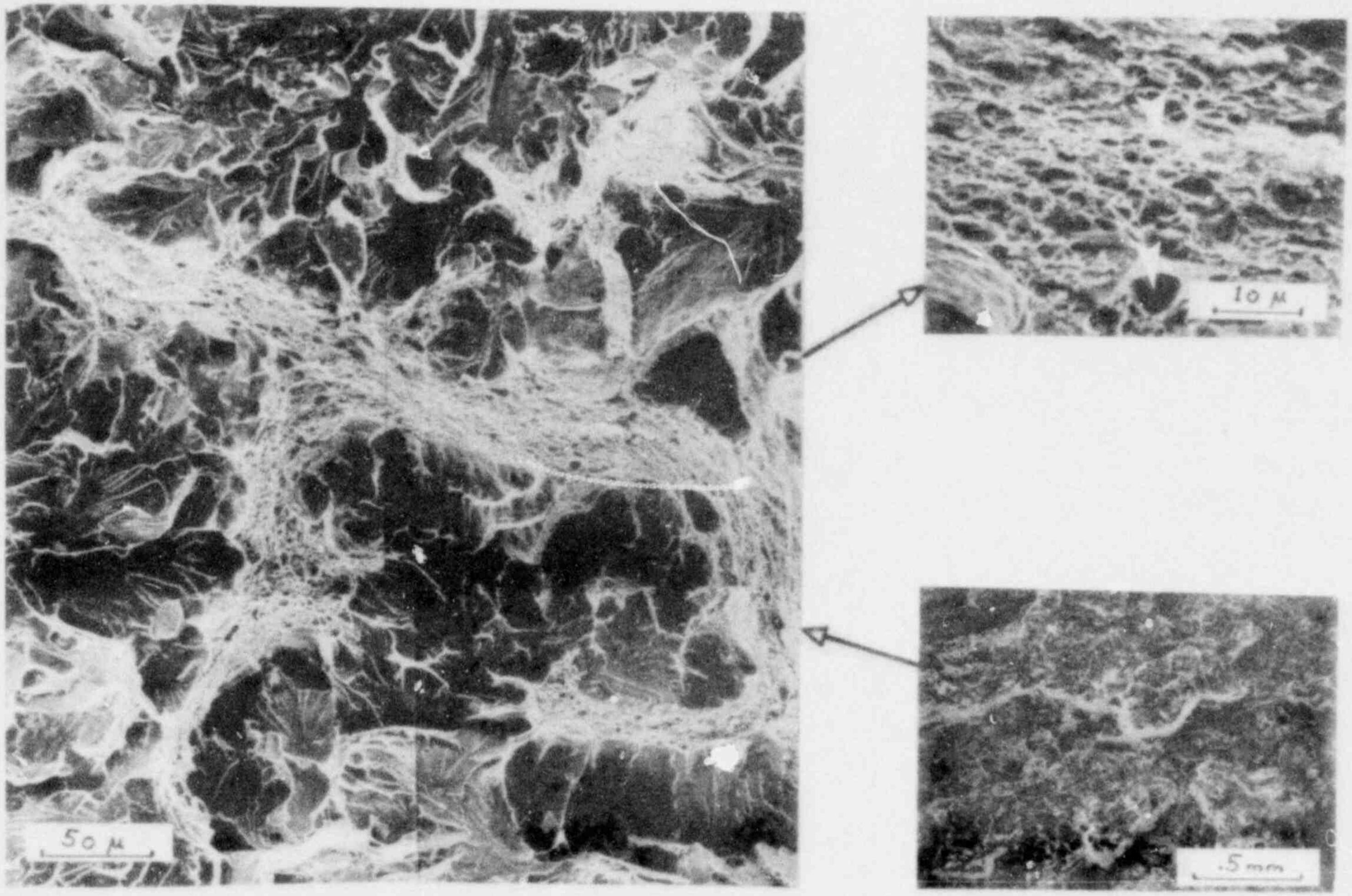

FIGURE 17. FRACTURE SURFACE OF CRACK ARREST SPECIMEN OF (D)A508 TESTED AT 39°C (ESTIMATED CRACK VELOCITY $\sim$500 ms^{-1}): LOWER RIGHT - LOW MAGNIFICATION SHOWING LIGAMENT; LEFT AND UPPER RIGHT - HIGHER MAGNIFICATION OF THE SAME AREA REVEALING DUCTILE SHEAR MODE OF LIGAMENT RUPTURE AND BRITTLE CLEAVAGE MODE OF SURROUNDING MATERIAL

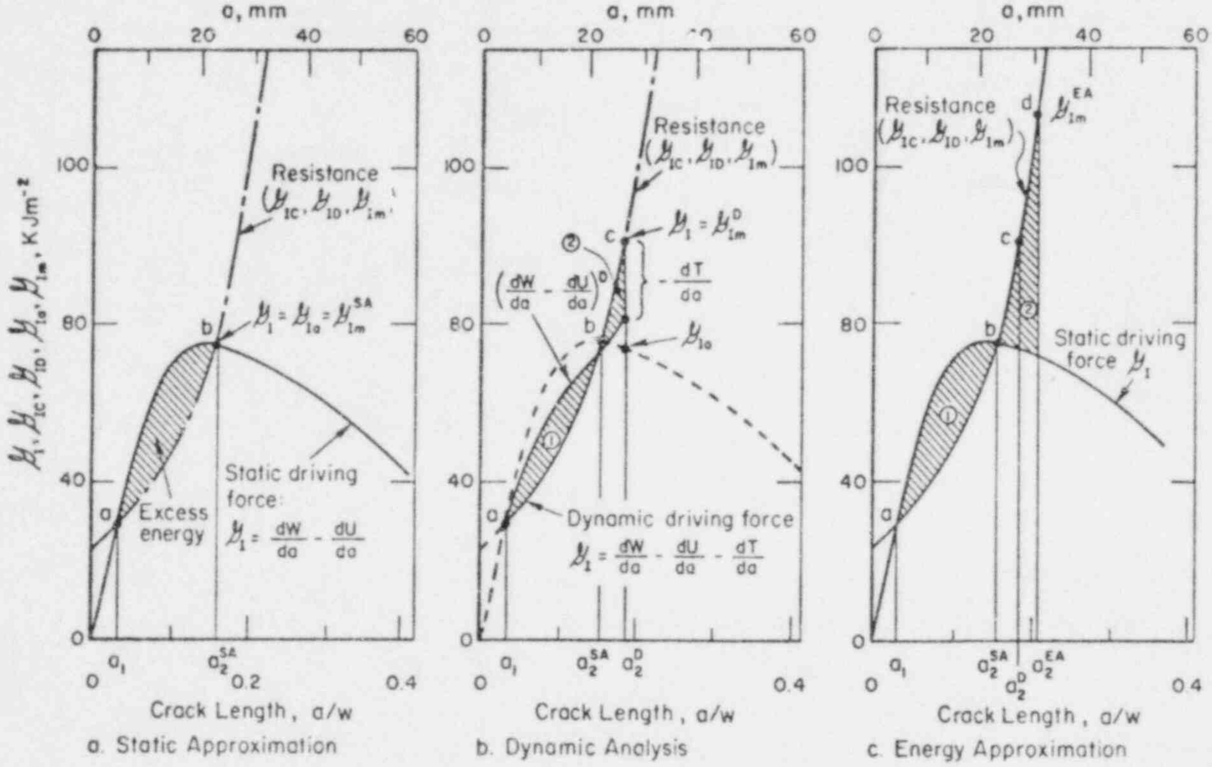

Figure 18. Schematic representation of the crack driving force ($\mathcal{G}_I$) and material fracture resistance ($\mathcal{G}_{Ic}$, $\mathcal{G}_{ID}$, $\mathcal{G}_{Im}$) in energy terms for the long axial surface flaw extending radially from the inner wall of a cylindrical vessel, corresponding to the stress intensity values given in Reference 62: (a) static approximation, (b) dynamic analysis, and (c) energy approximation. Note that a_1 is the initial crack length which is just unstable for the indicated driving force and resistance values; a_2 is the crack length of arrest, with the superscript SA, D, and EA referring to the static approximation, dynamic analysis and energy approximation. The scales on the ordinate and abcissa have been included to facilitate comparisons between $\mathcal{G}_I$ and K_I in Fig. 1, while the fracture resistance curve corresponds with the K_{Ic}, K_{ID}, K_{Im} curve in Fig. 1, it is strictly schematic and not a representative of a real material.